3/17/92

SIMULATION OF TWO-PHASE CARBON-14 TRANSPORT AT YUCCA MOUNTAIN, NEVADA

Mark D. White, Mark D. Freshley, and Paul W. Eslinger

Pacific Northwest Laboratory[a]
Richland, Wa.

Abstract

In support of Pacific Northwest Laboratory's (PNL) preliminary total system performance assessment of the proposed high-level nuclear-waste repository at Yucca Mountain, transport of carbon-14 (C^{14}) in the unsaturated zone was numerically modeled with the Multiphase Subsurface Transport Simulator (MSTS). Total system performance assessments are being conducted to estimate potential cumulative releases and doses from radionuclides being transported through different pathways to the accessible environment from the proposed waste repository. Transport of radionuclides in the gaseous and liquid phases are pathways through which some of the inventory in the proposed repository could reach the accessible environment. Carbon-14 transport in the unsaturated zone at Yucca Mountain was estimated with MSTS by considering two-phase diffusion, advection, phase partitioning, and radioactive decay. Transport results were based on a two-dimensional physical and hydrogeological system that represented an east-west cross section through Yucca Mountain. MSTS solves the nonlinear, partial-differential, conservation equations for water mass, air mass, and thermal energy with an implicit (i.e., forward time-differenced), finite-difference solution scheme. The nonlinearities in the governing partial-differential equations and corresponding finite difference forms are converted to linear form by the Newton-Raphson iteration technique. To compute species transport, MSTS solves a dilute species concentration conservation equation, which assumes that the species may be modeled as a passive scalar with respect to the other governing conservation equations. Liquid and gas-phase transport within the unsaturated zone were assumed to be driven by surface water recharge and radioactive-decay heat generation within the proposed repository. Carbon-14 source rates from failed repository waste canisters were estimated from the source term modeling subtasks associated with PNL's total system performance assessment of the proposed Yucca Mountain repository. Simulation results included estimates of liquid, gas, heat, and C^{14} transport within the unsaturated zone at Yucca Mountain. Predictions of C^{14} distributions surrounding the proposed nuclear waste repository within Yucca Mountain and a brief description of the thermal-hydrogeologic computer code MSTS are presented.

---

[a] Pacific Northwest Laboratory is operated by Battelle Memorial Institute for the U. S. Department of Energy under Contract DE-AC06-76RLO 1830.

Introduction

Yucca Mountain, Nevada, has been selected by the U.S. Department of Energy (DOE) as a potential site for construction of a proposed deep geologic repository for the permanent storage of high-level radioactive waste. The site is now being characterized (studied) to determine its suitability for waste storage. The strategy for site characterization has been outlined in the Site Characterization Plan (SCP; DOE 1988) by the DOE Office of Civilian Radioactive Waste Management (OCRWM). Data collected during the site characterization phase of repository analysis will be used to evaluate the performance of the proposed repository with respect to the statutory requirements of the Nuclear Waste Policy Act (Public Law 97-425), the Nuclear Waste Policy Amendments Act (Public Law 100-203), 10 CFR 60, and 40 CFR 191. DOE is required to submit a license application to the U.S. Nuclear Regulatory Commission (NRC).

Performance assessment analyses are being conducted on an ongoing basis to determine if unfavorable conditions exist that would preclude licensing a potential repository at Yucca Mountain. Performance assessment analyses also provide input to site characterization activities. To date, data collection activities conducted at Yucca Mountain provide initial estimates of hydraulic and geochemical properties. These initial estimates of Yucca Mountain properties provide the basis for OCRWM to begin development of performance assessment tools and strategies that will be used in the license submittal to NRC. Of primary importance are conceptual and numerical models that increase the current understanding of conditions at Yucca Mountain and provide direction to the field and laboratory activities described in the SCP.

As part of the studies at Yucca Mountain, the Yucca Mountain Site Characterization Project Office is conducting a series of Total Systems Performance Assessment (TSPA) exercises. The TSPA exercises are intended to provide opportunities to evaluate and review the capabilities to predict the performance of the geologic repository over a period of 10,000 years after waste emplacement. A principal concern of performance assessment involves the prediction of cumulative radionuclide releases to the accessible environment and radiation doses received by individuals in the accessible environment. Radioactive carbon-14 (C^{14}) has been included among the listed radionuclides that will be considered for predicting cumulative radionuclide releases. Predictions of cumulative radionuclide releases require predictions of radionuclide transport from the waste package canister to the accessible environment. This paper describes the simulations of C^{14} transport from the proposed repository horizon to the ground surface and water table for specified C^{14} source rates, repository thermal loadings and prescribed hydrogeologic properties for the vadose zone. Because C^{14} would exist as gaseous carbon-dioxide and dissolved carbonate in the aqueous phase, C^{14} transport at Yucca Mountain was numerically modeled as a two-phase system.

Previous predictions of C^{14} migration at Yucca Mountain (Ross 1988) have been restricted to gas-phase migration under steady-state conditions. The predictions reported in this paper consider the transient transport of C^{14} within both the aqueous and gas phases, for a two-dimensional domain, over a period of 10,000 years after waste emplacement. The thermal and hydrogeologic fields within the computational domain were computed based on steady-state surface recharge rates and the transient design basis thermal loading for the proposed repository.

This paper gives a brief site description, followed by an overview of the numerical model Multiphase Subsurface Transport Simulator (MSTS), which generated the reported simulation results. An overview discussion of the results are preceded with a problem description in terms of the physical and computational domains and the hydrogeological system. The paper concludes with a discussion of physical and numerical assumptions and a perspective on future prediction techniques.

Site Description

Yucca Mountain consists of a thick sequence of both welded and nonwelded volcanic tuffs that dip 5 to 10 degrees to the east (Montazer and Wilson 1984). The tuffs form a thick

unsaturated zone and extend well below the water table. The densely welded tuffs are typically highly fractured with low saturated matrix hydraulic conductivities (Peters and Klavetter 1988). The nonwelded tuffs that are vitric have few fractures and relatively high saturated matrix hydraulic conductivities, while the zeolitic nonwelded tuffs are characterized by relatively few fractures and low matrix hydraulic conductivities. The unsaturated zone at Yucca Mountain is characterized by a low recharge rate. The fractures present in the welded and nonwelded tuffs at Yucca Mountain represent heterogeneities where the flow properties vary by several orders of magnitude, depending on the local hydraulic conditions. Current designs for the proposed geologic repository locate the underground facilities within the vadose zone, approximately 450 m below the mountain ridge and 250 m above the water table. This repository horizon positions the proposed underground facilities primarily in the welded tuff of the Topopah Springs Member.

Numerical Model

Computer codes that simulate transport processes in geologic media are typically classified according to capabilities related to phases, components, saturations, transport and dimensionality. Under this classification strategy, MSTS would be classified as a two-phase, two-component, three-dimensional numerical simulator, for variably saturated geologic media, with dilute species transport capabilities. This classification arises because MSTS models two phases (liquid and gas), two components (water and air), and solves equations for dilute species transport through variably saturated geologic media. MSTS uses a finite-difference based numerical scheme to solve a nonlinear system of conservation and constitutive equations. The conservation equations in partial differential form for the conservation of water mass, air mass, thermal energy, and species concentration (Equations 1 through 4) appear as follows:

$$\frac{\partial}{\partial t}[n_d\, y_w\, \rho_l\, s_l + n_d\, x_w\, \rho_g\, s_g] = \nabla\left[\frac{y_w\, \tilde{k}\, k_{rl}\, \rho_l}{\mu_l}\left(\nabla P_l + \rho_l\, g\, \hat{z}\right)\right] + \nabla\left[\frac{y_w\, \tilde{k}\, k_{rg}\, \rho_g}{\mu_g}\left(\nabla P_g + \rho_g\, g\, \hat{z}\right) + \tau_g\, n_d\, \rho_g\, s_g\, D_{aw}\, \nabla x_w\right] + \dot{m}_w \tag{1}$$

$$\frac{\partial}{\partial t}[n_d\, y_a\, \rho_l\, s_l + n_d\, x_a\, \rho_g\, s_g] = \nabla\left[\frac{y_a\, \tilde{k}\, k_{rl}\, \rho_l}{\mu_l}\left(\nabla P_l + \rho_l\, g\, \hat{z}\right)\right] + \nabla\left[\frac{y_a\, \tilde{k}\, k_{rg}\, \rho_g}{\mu_g}\left(\nabla P_g + \rho_g\, g\, \hat{z}\right) - \tau_g\, n_d\, \rho_g\, s_g\, D_{aw}\, \nabla x_w\right] + \dot{m}_a \tag{2}$$

$$\frac{\partial}{\partial t}\left[\frac{(1 - n_t)\, \rho_s\, u_s + \eta_d\, \rho_l\, u_l + n_d\, s_g\, \rho_g\, u_g}{\partial t}\right] + \nabla[\rho_l\, h_l\, V_l + \rho_g\, h_g\, V_g] = \nabla\left[\left[\tilde{k}_e + n_d\, \rho_l\, c_l\, \tilde{D}_l\right] \nabla T\right] + \dot{q} + h_w \dot{m}_w + h_a \dot{m}_a \tag{3}$$

$$\frac{\partial C}{\partial t} + \nabla[C_l\, V_l + C_g\, V_g] = \nabla\left[\tau_l\, s_l\, n_d\, \dot{D}_{cl}\, \nabla C_l + \tau_g\, s_g\, n_d\, \dot{D}_{cg}\, \nabla C_g\right] + \dot{s}_c - \dot{R}_c\, C \tag{4}$$

The water and air mass conservation equations were written to include Darcy flow for both phases and binary diffusion of water vapor and gaseous air for the gas phase. Molecular diffusion of dissolved air in the liquid phase is ignored. The thermal energy conservation equation includes heat transfer through advection of fluids for both phases and heat transfer by conduction through the solid and liquid phases. A mechanical dispersion coefficient may be invoked to model the phenomena of kinematic dispersion, which occurs because of the heterogeneity of the microscopic velocities within the porous medium. Heat transfer by conduction and heat transfer by binary diffusion within the gas phase have been ignored.

MSTS allows for multiple porosities: total porosity, diffuse porosity, and effective porosity. The total porosity represents the entire fractional pore space within the geologic medium. The diffuse porosity accounts for the fractional pore space that is connected, and the effective porosity represents the diffusive porosity less the fractional pore space occupied by the residual moisture.

The species concentration conservation equation includes species transport by advection and diffusion for both phases. As with the thermal energy conservation equation, a mechanical dispersion coefficient may be specified to model kinematic dispersion. Radioactive decay of the species concentration may be modeled, without tracking decay products.

The primary dependent variables for the water mass, air mass, thermal energy, and species concentration conservation equations are, respectively: liquid pressure, gas pressure, temperature, and species concentration. The constitutive equations are complex expressions that relate the primary dependent variables to the secondary variables that appear as coefficients in the governing conservation equations. The nonlinear dependencies of the secondary variables on the primary dependent variables yield nonlinearities in the finite-difference based algebraic expressions of the governing conservation equations. The constitutive equations may be lumped into two categories, physical property relationships and hydrogeologic relationships. The physical property relationships provide dependencies for the primary dependent variables to physical properties such as density, viscosity, internal energy, enthalpy, saturation pressures, and component mass fractions for both phases. Water physical properties are computed from ASME steam table functions (ASME 1967); whereas, air physical properties are computed from empirical functions and the ideal gas law. Gas-phase properties are computed by combining air and water vapor physical properties through either Dalton's partial pressure ideal gas laws, or from the relationships for the kinetic theory of gas mixtures. The hydrogeologic constitutive equations relate the primary dependent variables to hydrogeologic characteristic and transport properties such as liquid and gas saturations, phase relative permeabilities, and effective thermal conductivity. The hydrogeologic constitutive equations are generally based on empirical and semi-empirical relationships.

The governing conservation equations are solved by discretizing their partial differential forms with a finite-difference scheme. Spatial discretization is currently limited to multi-dimensional, regular and irregular, Cartesian or cylindrical grid systems, where the cylindrical grid systems are limited to cylinders aligned with the gravitational field. Temporal discretization is fully-implicit. Interface diffusion conductances, such as hydraulic and thermal conductivities, may be specified with arithmetic, geometric, or harmonic means or an upwind weighting scheme. Geometric mean interface diffusion conductances were used for the reported simulations. The water and air mass conservation equations use upwind weighting for the diffused densities. The advection terms of the thermal energy conservation equation are formulated with an upwind weighting scheme for the advected properties; whereas, the species conservation equation combines the advection and diffusion terms with a Peclet number dependent power-law scheme (Patankar 1980) formulated for two-phase flow. The two-phase power-law scheme for combining the advection and diffusion components of the species conservation equation is shown in Equations 5 through 7 for a single dimension; where a_e represents the transport coefficient for the neighboring cell at the upper node index, a_w represents the transport coefficient for the neighboring cell at the lower node index, and a_p represents the transport coefficient for the local cell.

The dilute concentration assumption associated with the species conservation equation implies that the species responds as a passive scalar with respect to the other governing equations.

$$a_e = D_{l_e}\left[\left[0,\left(1-\frac{0.1|F_{l_e}|}{D_{l_e}}\right)\right]\right] + [[0,-F_{l_e}]] + D_{g_e}\left[\left[0,\left(1-\frac{0.1|F_{g_e}|}{D_{g_e}}\right)\right]\right] + [[0,-F_{g_e}]] \quad (5)$$

$$a_w = D_{l_w}\left[\left[0,\left(1-\frac{0.1|F_{l_w}|}{D_{l_w}}\right)\right]\right] + [[0,F_{l_w}]] + D_{g_w}\left[\left[0,\left(1-\frac{0.1|F_{g_w}|}{D_{g_w}}\right)\right]\right] + [[0,F_{g_w}]] \quad (6)$$

$$a_p = a_e + a_w + F_{l_e} + F_{g_e} - F_{l_w} - F_{g_w} \quad (7)$$

That is, the physical and transport properties of the other governing equations are assumed to be independent of species concentrations. This assumption allows the species conservation equation to be decoupled and solved independently from the other governing equations. The finite-difference forms of the governing equations for water mass, air mass, and thermal energy are solved simultaneously in an iterative scheme. The nonlinear finite-difference equations are converted to a linear form, and solved iteratively following the Newton-Raphson technique for multiple variables. The computed gas- and liquid-phase flow fields, from a converged solution for the coupled mass and heat transport equations, are then applied to the solution of the species transport equations. For single-phase, nonisothermal flow problems only the water mass and thermal energy transport equations are solved in a coupled manner. Likewise, for single-phase, isothermal flow problems only the water mass transport equation is solved.

Physical and Hydrogeological System

The physical and hydrogeological system relevant to the Yucca Mountain TSPA exercises consisted of a two-dimensional domain divided into five hydrogeologic strata, as shown in Figure 1. The physical domain extended vertically from the water table to the ground surface, and horizontally as an east-west transect that extended from borehole USW H-5 at the crest of Yucca Mountain to roughly 500 m east of borehole UE-25a#1. The repository is illustrated by a downward sloping line at elevations of 1030 m beneath the crest of Yucca Mountain and 895 m at the eastern facility boundary. The repository horizon was modeled using the thermal and hydrogeological transport properties of welded tuff with a decaying internal heat generation source. Heat generation was computed assuming a design repository loading (Schelling 1987) of 49.9 MTHM/acre composed of 40% 27,500 MWd/MTHM BWR fuel and 60% 33,000 MWd/MTHM PWR fuel (5 yr spent fuel); thus, producing an initial heat source of roughly 67 kW/acre.

The computational model used to simulate the physical domain was structured on a uniform two-dimensional Cartesian grid with 50 rows and 94 columns. The vertical and horizontal grid dimensions were uniform over the computational domain at 15 and 30 m, respectively. Of the 4700 nodes within the computational domain 776 nodes were treated as noncomputational nodes, which yields 3924 active computational nodes. The noncomputational nodes were used to generate the irregular boundary of the Yucca Mountain ground surface with a stair-stepped approach.

The water table was modeled as a saturated boundary for the liquid phase, a zero flux boundary for the gas phase, a constant temperature boundary (30°C) for heat transport, and a zero C^{14} concentration boundary for species transport. The ground surface was modeled with "stair stepped" horizontal boundaries with, specified uniform liquid recharge rates for the liquid phase, standard atmospheric gas pressures for the gas phase, 10% relative humidity for vapor binary diffusion, a constant temperature boundary (20°C) for heat transport, and a zero C^{14} concentration boundary for species transport. Vertical boundaries were modeled as zero flux boundaries. Initial conditions were those computed for steady-state saturation conditions with the applied surface recharge and reported Yucca Mountain geothermal gradient (Schelling 1987).

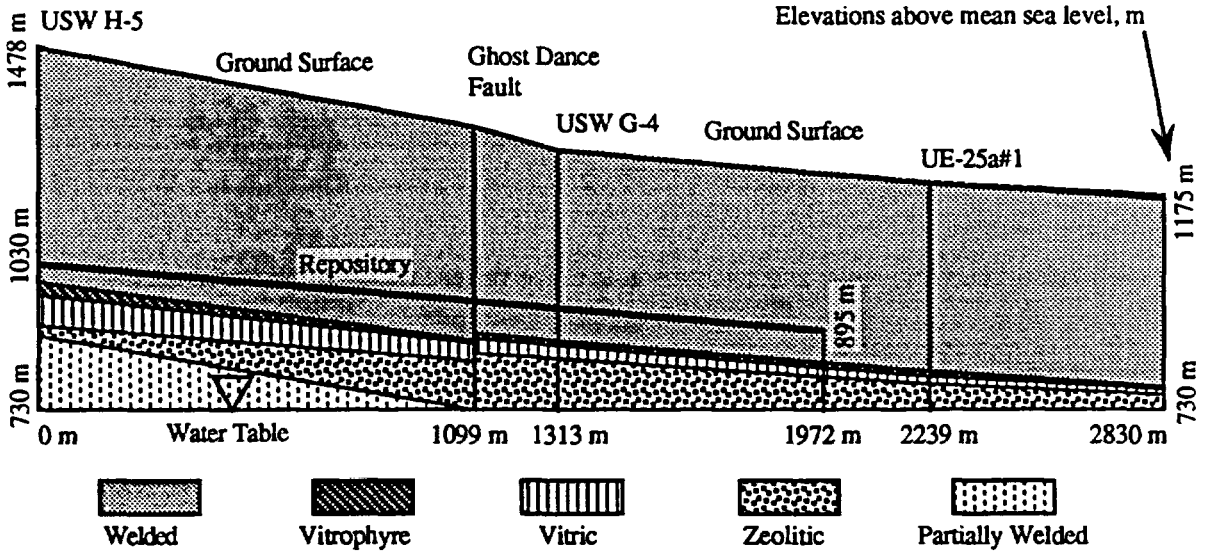

FIGURE 1. East-West Cross Section: Physical and Hydrogeologic System

The hydrogeologic stratigraphy shown in Figure 1 and the hydrogeologic properties associated with tuff layer were specified in conjunction with the Yucca Mountain TSPA exercises[b]. The data were reported separately for matrix and fracture properties as shown in Tables 1 and 2. Matrix properties were derived from Peters et al. (1984) and fracture properties were derived from Carsel and Parish (1988) and Spengler et al. (1984).

TABLE 1. Matrix Hydrogeologic Properties

Tuff	Hydraulic	van Genuchten Parameters			
Layer	Conductivity, m/s	α, 1/m	β	S_r	Porosity
Welded	2.00×10^{-11}	0.0057	1.798	0.080	0.11
Vitrophyre	3.01×10^{-11}	0.0033	1.798	0.052	0.09
Vitric	7.99×10^{-11}	0.0265	2.223	0.164	0.21
Zeolitic	3.01×10^{-11}	0.0220	1.236	0.010	0.41
Partially Welded	1.40×10^{-8}	0.0140	2.640	0.066	0.24

TABLE 2. Fracture Hydrogeologic Properties

Tuff	Hydraulic	van Genuchten Parameters			
Layer	Conductivity, m/s	α, 1/m	β	S_r	Porosity
Welded	8.25×10^{-5}	14.5	2.68	0.10465	0.00663
Vitrophyre	8.25×10^{-5}	14.5	2.68	0.10465	0.00835
Vitric	8.25×10^{-5}	14.5	2.68	0.10465	0.00047
Zeolitic	8.25×10^{-5}	14.5	2.68	0.10465	0.00038
Partially Welded	8.25×10^{-5}	14.5	2.68	0.10465	0.01032

[b] Letter report from P. Kaplan, G. Gainer, H. Dockery, and R. Barnard, Sandia National Laboratories, Albuquerque, New Mexico, July 25, 1991. Distributions of Hydrogeologic Parameters for the TSA problem.

Matrix and fracture hydrogeologic properties were combined, using a dual-porosity model, to form equivalent continuum properties for each tuff layer. Equivalent continuum models represent the combined effects of the matrix and fracture properties through equivalent bulk properties, with the primary assumption of pressure equilibrium between the medium matrix and fractures. The equivalent continuum relations for bulk saturation, saturated hydraulic conductivity, and liquid relative permeability are shown in Equations 8 through 10, respectively. Bulk gas-phase relative permeabilities were assigned a value of 1.0 minus the liquid-phase relative permeability. Tortuosities, shown in Equations 11 and 12, were computed from the bulk properties for porosity and phase saturation using the saturation dependent formulation developed by Millington and Quirk (1959).

$$s_{lb} = \frac{s_{lm}(1 - n_f)\, n_m + s_{lf}\, n_f}{(1 - n_f)\, n_m + n_f} \tag{8}$$

$$k_b = k_m(1 - n_f) + k_f\, n_f \tag{9}$$

$$k_{rlb} = \frac{k_m\, k_{rlm}(1 - n_f) + k_f\, k_{rlf}\, n_f}{k_b} \tag{10}$$

$$\tau_l = n_d^{10/3}\, s_f^{4/3} \;,\; \tau_g = n_d^{10/3}\, s_g^{4/3} \tag{11,12}$$

The Yucca Mountain tuff layers are characterized by small pore sizes and large matric potentials under low liquid saturation conditions. Because of the local desaturation, which would occur around the repository after waste emplacement, the phenomena of vapor pressure lowering was included in the reported simulations. Vapor pressure lowering, as shown in Equation 13, is an experimentally observed phenomena (Nitao 1988) which effectively lowers the vapor pressure above the pore water; i.e., raises the pore water boiling point.

$$P_v = P_{sat}\, exp\left(\frac{-P_c}{\rho_l\, R_l\, T}\right) \tag{13}$$

The transport of C^{14} within the vadose zone at Yucca Mountain is strongly dependent on complex geochemical interactions and equilibrium conditions. Equilibrium conditions for C^{14} between the gas, aqueous, and solid phases will depend on the local thermal, hydrogeological, and geochemical environment. For the reported simulations, C^{14} equilibrium conditions were computed in terms of a partition coefficient, based on a temperature-dependent carbon equilibrium model developed by Amter et al. (1988) for estimates of the geochemical conditions in the unsaturated zone at Yucca Mountain. Amter's geochemical model predicts a partition coefficient that expresses carbon equilibrium conditions between carbon dioxide in the gas-phase and dissolved carbonates in the aqueous phase. The model predicts liquid- and gas-phase concentrations of carbonate species at 27°C equal to 1.3 mmol/L and 0.04 mmol/L, respectively. Lower ratios of liquid- to gas-phase concentrations would occur at higher temperatures. Partitioning between the liquid- and solid-phase has been ignored for the reported simulations.

Simulation Results

Two calculations were performed that varied in surface recharge rates and waste package failure times. Because waste package failure times were not coordinated with the thermal and hydrogeologic histories computed by these calculations, these calculations should only be considered as exemplar with respect to predicting total system performance. In the first simulation constant surface recharge rate of 0.0 mm/yr was assumed over the entire 10,000-year simulation period. The waste canister failures were assumed to occur such that a constant release rate of C^{14} was produced over the period from 2,000 to 5,000 years. In the second simulation a constant surface recharge rate of 0.01 mm/yr was assumed over the entire 10,000-year simulation period. For the higher surface recharge simulation, waste canisters were assumed to fail over a period from 300 to 10,000 years. Carbon-14 releases from the waste canisters for the zero recharge case were assumed to occur as instantaneous releases to the gas phase following a waste package failure. Conversely for the 0.01 mm/yr recharge case, instantaneous gas releases of C^{14} were assumed to precede limited releases to the aqueous phase. Chemical and isotopic equilibrium between the carbon element existing as carbon dioxide in the gas phase and carbonate in the aqueous phase were assumed; therefore, release modes were essentially ignored, except for timing and rates.

The calculation period starts after waste emplacement boreholes, repository drifts, and access boreholes have been completely backfilled. Emplacement histories and operational conditions have been ignored. The ambient thermal and hydrogeological conditions surrounding the repository were assumed to be those of the undisturbed saturation fields and geothermal gradients. After 100 years, the simulated thermal and liquid saturation fields surrounding the repository are computed to have changed for the zero recharge case (Figures 2 and 3). The repository reached peak temperatures, and boiling of the water immediate to the repository has resulted in a relatively dry region within and immediately adjacent to the repository. Water evaporated from the repository recondensed beyond the desaturated zones. This structure of a high temperature desaturated zone adjacent to a cooler saturated zone produces a dynamic heat pipe (counter-current gas- and liquid-phase flows), which greatly increases heat transfer rates away from the repository. Such heat pipe flow is considered dynamic because the heat pipe location migrates relative to the repository during the thermal transient. Accumulated water at the outer boundaries of the heat pipe zone starts to travel down the sloped repository at fracture flow rates.

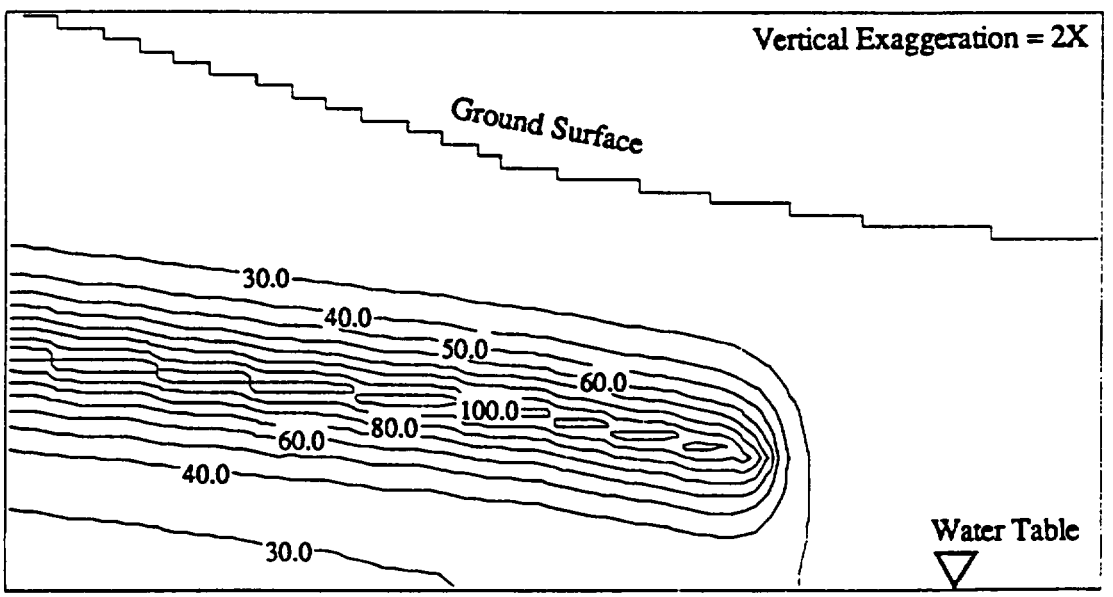

FIGURE 2. Temperature Contours,°C (at 100 yrs, 0.0 mm/yr Recharge Case)

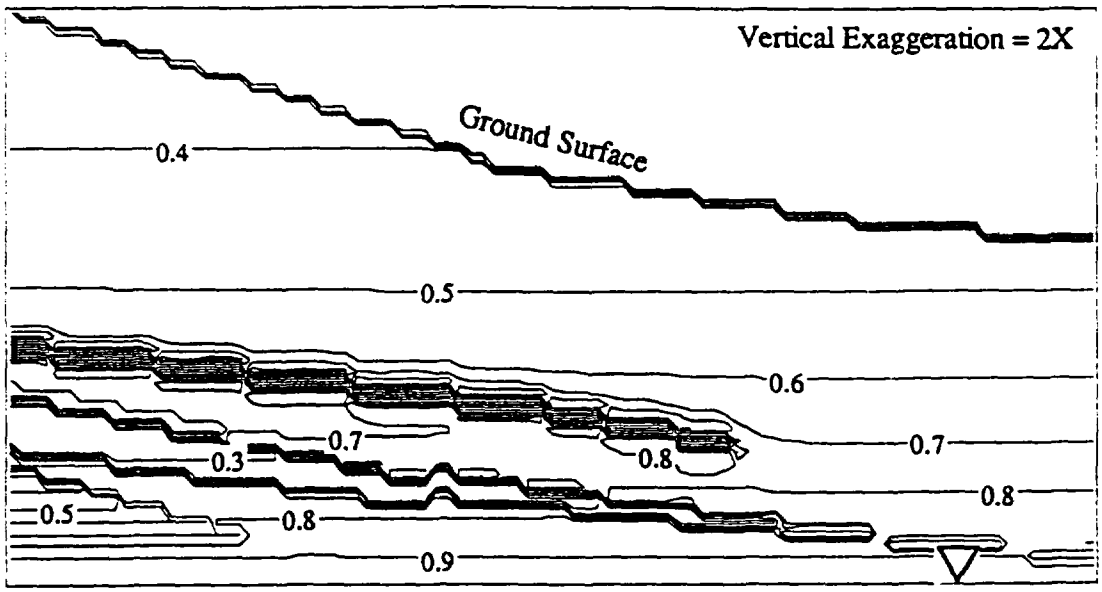

FIGURE 3. Liquid Saturation Contours (at 100 yrs, 0.0 mm/yr Recharge Case)

After 2,000 years, simulation results predict temperature and liquid saturation fields will have decayed considerably from their peak temperature structures (Figures 4 and 5). Maximum temperatures of 68.5°C, which are predicted along the repository horizon, are insufficient to sustain the heat pipe flow structures observed at earlier times. The steep liquid saturation gradients observed around the repository at 100 years disappeared at 2,000 years, and the repository horizon has nearly resaturated to the initial state. After 3,000 years, the waste canisters were assumed to have been failing in a uniform fashion along the repository horizon, which created a constant C^{14} release rate. Fields of C^{14} concentrations at 3,000 and 10,000 years

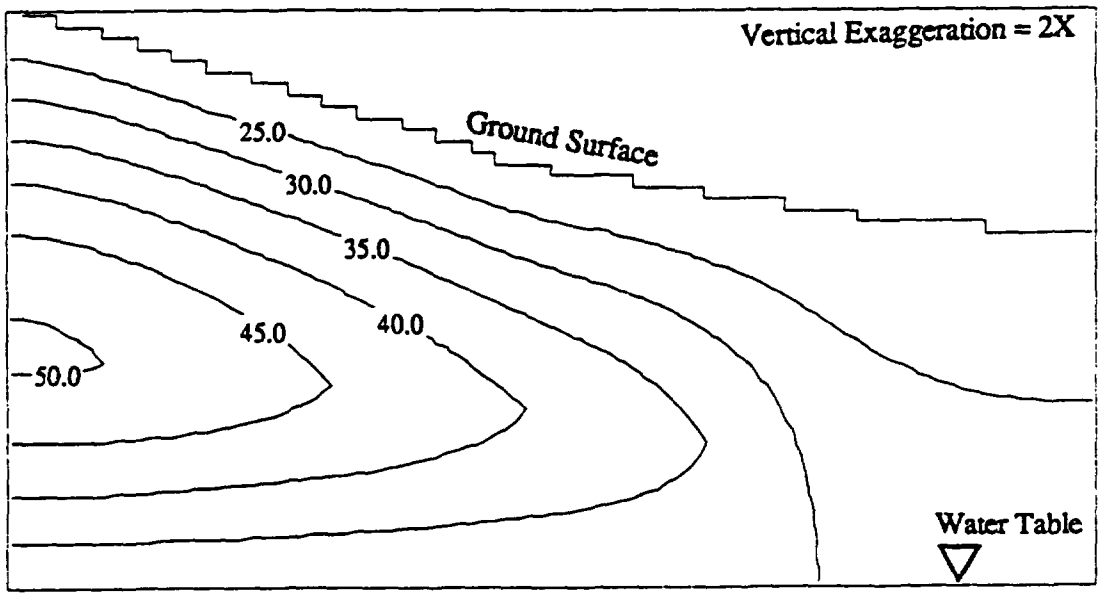

FIGURE 4. Temperature Contours,°C (at 2000 yrs, 0.0 mm/yr Recharge Case)

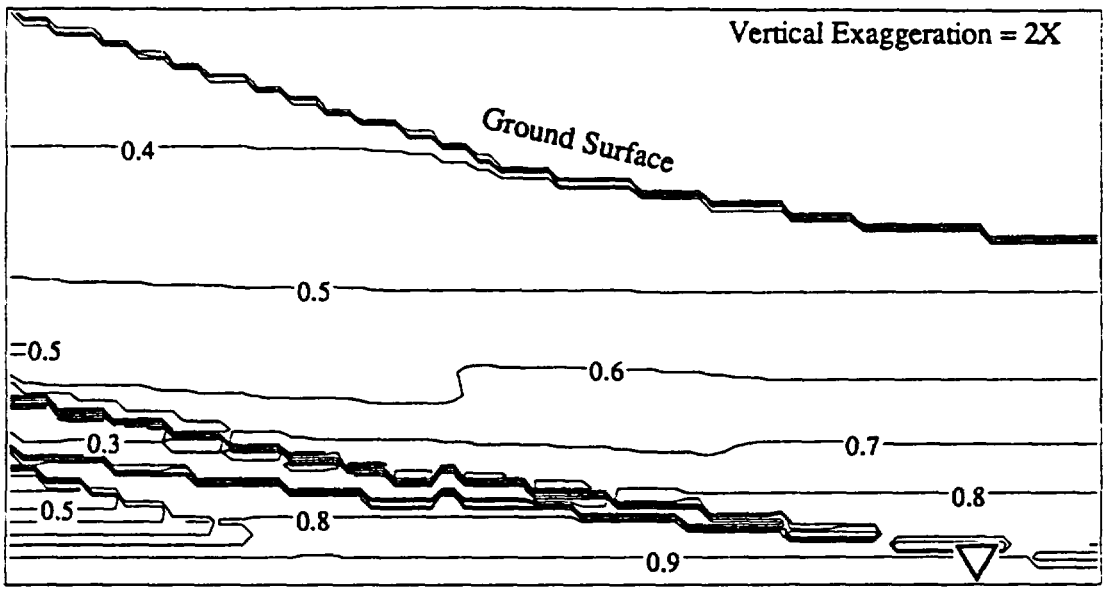

FIGURE 5. Liquid Saturation Contours (at 2000 yrs, 0.0 mm/yr Recharge Case)

(Figure 6 and 7) display classical diffusion-type transport of C^{14} towards the groundwater and ground surface. The peak C^{14} concentrations near the eastern end of the repository horizon at 3,000 years result from the higher local saturations generated during the thermal transient period. Although C^{14} transport was modeled considering both advection and diffusion transport processes in the gas and aqueous phases the dominate mode of transport for the physical system described by this TSPA exercise was by diffusion through the gas phase.

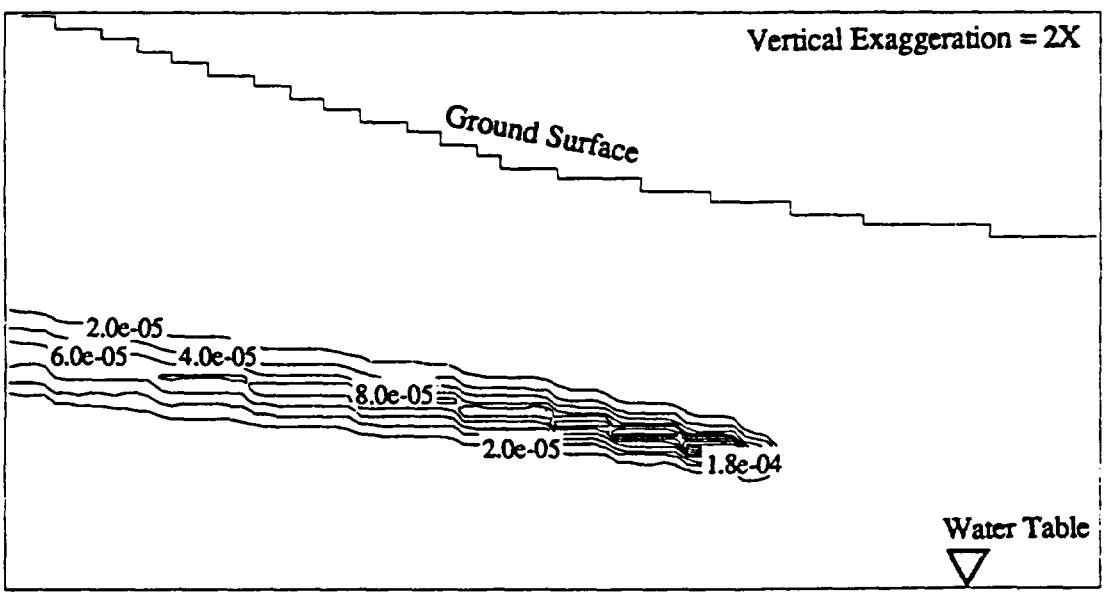

FIGURE 6. C^{14} Concentration Contours, Ci/m^3 (at 3000 yrs, 0.0 mm/yr Recharge Case)

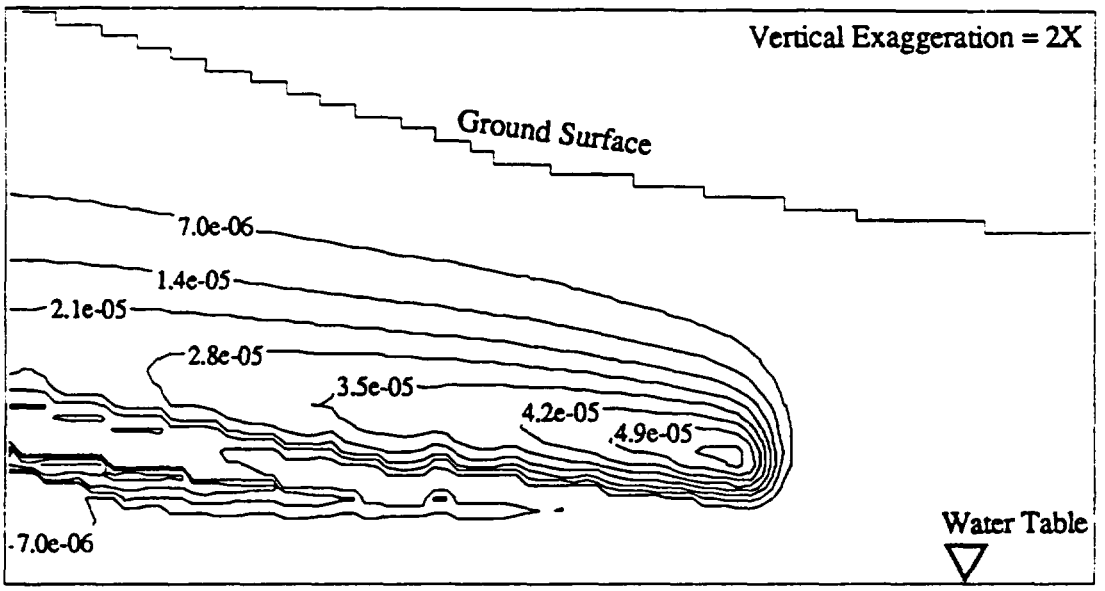

FIGURE 7. C^{14} Concentration Contours, Ci/m^3 (at 10,000 yrs, 0.0 mm/yr Recharge Case)

The simulation results for the 0.01 mm/yr recharge case qualitatively resemble those for the zero recharge case. The primary difference between the two simulations results from the generally higher liquid saturations from surface recharge. Higher initial saturations around the repository resulted in lower peak temperatures and increased migration of liquid water down the slope of the repository horizon. Because higher saturations decrease gas phase transport of C^{14}, concentration profiles of C^{14} for the 0.01 mm/yr recharge case were significantly narrower along the repository. With respect to C^{14} transport to the groundwater or ground surface, the net result of the higher recharge rate was to reduce releases. Because the geochemical equilibrium state for C^{14} within the vadose zone at Yucca Mountain puts nearly 97% of the carbon element by volume into the aqueous phase, higher recharge rates could result in increased C^{14} transport to the groundwater. Releases to the groundwater could become significant if fracture pathways participate in the aqueous-phase migration.

Quantitative comparisons of the two simulated TSPA exercise cases are shown in terms of C^{14} transport to the ground surface and water table in Figures 8 and 9. Cumulative canister releases represent the total amount of C^{14} released from the failed waste canisters into the system reduced by the amount of C^{14} depleted through radioactive decay and the amount of C^{14} leaving the system by crossing the surface or groundwater boundaries. Travel times and transport rates for the migration of C^{14} to the surface and groundwater were predicted to be greater for the 0.0 mm/yr case versus the 0.01 mm/yr case, because of the higher liquid saturation levels observed for the higher recharge case.

Assumptions and Conclusions

The current Yucca Mountain TSPA exercises were designed to evaluate the execution of various numerical models to perform calculations in support of site performance issues related to licensing regulations. These exercises were intended to be iterative where results, peer review, new field data, and experimental tests would guide the refinement and application of the numerical models. Because several independent investigations are occurring concurrently on each aspect of system performance, there are different numerical methods for predicting performance, which allow benchmarking comparisons. The final performance calculations related to site licensing will

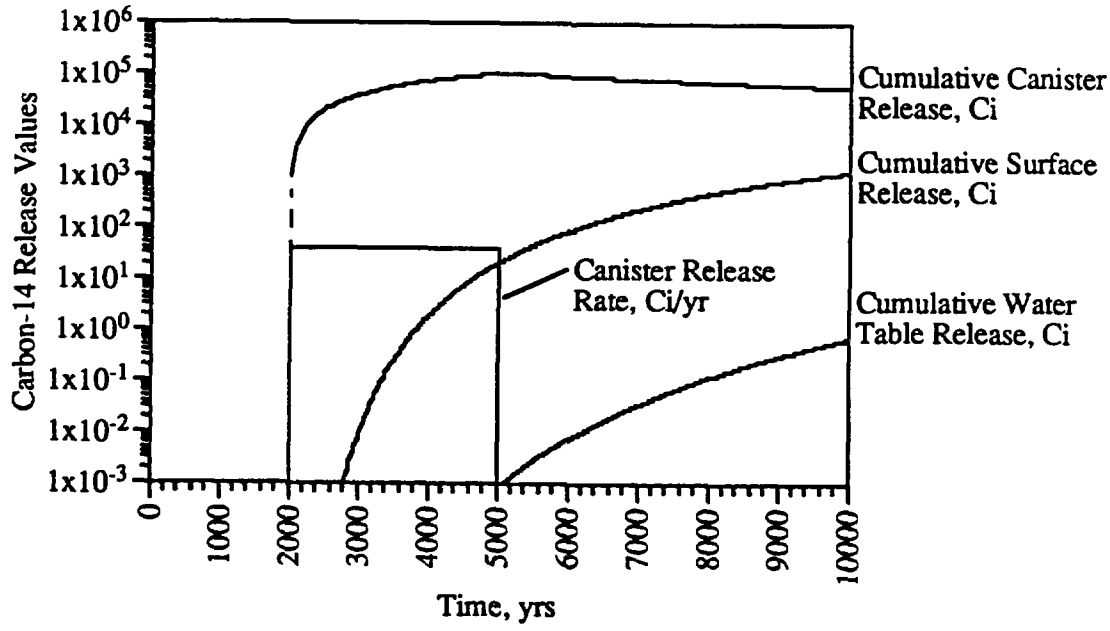

FIGURE 8. C^{14} Release Histories, 0.0 mm/yr Recharge Case.

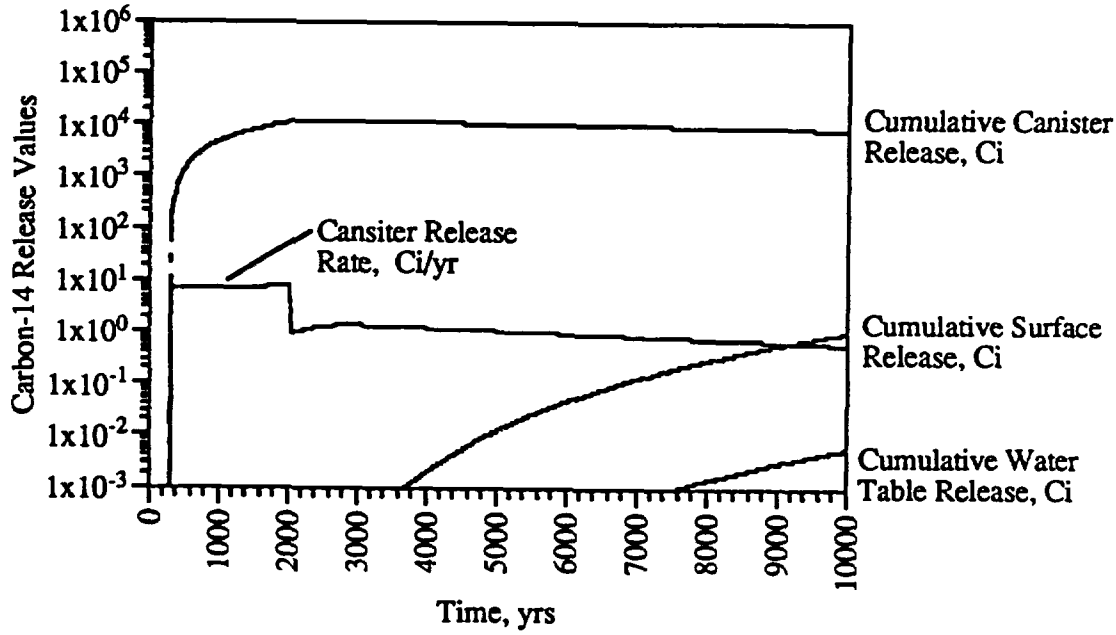

FIGURE 9. C^{14} Release Histories, 0.01 mm/yr recharge case.

represent the culmination of information and experience gained during these preliminary performance assessment exercises. Because of the iterative nature of these exercises, no specific conclusions will be drawn on the cumulative releases of C^{14} or doses to the accessible environment. Instead, a discussion of modeling and physical assumptions is offered, with emphasis on C^{14} transport within the vadose zone at Yucca Mountain.

Yucca Mountain's topography, hydrogeologic stratigraphy, and proposed repository composes a complex three-dimensional system. The surface of Yucca Mountain has differing east and west slopes, with numerous washes. The mountain is composed of highly fractured tuff layers with contrasting and heterogeneous properties, which are transected with various faults that include local faults related to the formation of calderas and longer faults of the basin-and-range type. Although incomplete, the repository conceptual design involves a network of drifts, emplacement panels, and boreholes large enough to accommodate the equivalent of 70,000 MTHM. The two-dimensional system modeled here ignores all three-dimensional aspects of the physical system, and the coarse mesh, designed for investigating far-field transport is incapable of capturing repository-scale phenomena. For example, reported peak repository temperatures of 108°C are considerably lower than those reported from canister-scale thermal and hydrogeologic models. These lower temperatures are primarily due to the application of repository decay heat powers over larger volumes than those for individual waste canisters. Another critical modeling assumption was to neglect the Ghost Dance Fault.

The primary assumption associated with the equivalent continuum model for fracture and matrix flow through partially saturated porous media is that pressure equilibrium occurs between the fracture and matrix over times sufficiently shorter than the time constants for the flow phenomena of interest. Recent research by Nitao and Buscheck (1989) have shown that this assumption may be inconsistent with the fracture flow phenomena within Yucca Mountain. One other assumption associated with the equivalent continuum model that may prove inconsistent with experimental data is that the fractures are sufficiently random in orientation to be considered isotropic.

Because of the saturation-dependent tortuosities used for the reported simulations, gas-phase diffusion of C^{14} was strongly dependent on the saturation fields. Simulations of repository performance at higher recharge rates predicted lower gas-phase transport of C^{14}, because of the inhibition of gas-phase advection and diffusion by the liquid saturation barrier surrounding the repository. The accuracy of saturation-dependent tortuosities relative to gas-phase diffusion of C^{14} in the vadose zone at Yucca Mountain is not completely known.

The spatial and temporal extent of the thermally driven liquid saturation field surrounding the repository is critical to predicting canister failures and radionuclide transport. Capillary hysteresis has been ignored, but may prove to be a critical phenomena for predicting saturation fields immediate to the repository because of the drying and rewetting events produced by the thermal transient. Vapor pressure lowering, a model used for the reported results, effectively lowers peak temperatures and limits pore desaturation. Because the vapor pressure lowering model was based on experiments conducted at room temperature, it may significantly over predict the amount of absorbed water. To accurately model this phenomena temperature-dependent water retention characteristic data would be required.

Nomenclature

Roman Characters

C	species concentration, (mol,Ci)/m^3
C_g	gas-phase species concentration, (mol,Ci)/m^3 gas
C_l	liquid-phase species concentration, (mol,Ci)/m^3 liquid
c_l	liquid-phase specific heat, J/kg K
D_l	liquid mechanical dispersion coefficient, m^2/s
D_{cg}, D_{cl}	gas species diffusion coefficient, liquid species diffusion coefficient, m^2/s
D_{ge}, D_{le}	gas diffusion coefficient upper face, liquid diffusion coefficient upper face, m/s
D_{gw}, D_{lw}	gas diffusion coefficient lower face, liquid diffusion coefficient lower face, m/s
F_{ge}, F_{le}	gas advection coefficient upper face, liquid advection coefficient upper face, m/s
F_{gw}, F_{lw}	gas advection coefficient lower face, liquid advection coefficient lower face, m/s

g	acceleration of gravity, m/s^2
h_a, h_w	air enthalpy, water enthalpy, J/kg K
h_g, h_l	gas enthalpy, liquid enthalpy, J/kg K
k	intrinsic permeability, bulk, matrix, fracture, m^2
k_e	equivalent thermal conductivity, W/m K
k_{rg}, k_{rl}	gas relative permeability, liquid relative permeability
$\dot{m}_w$, $\dot{m}_a$	air mass source, water mass source, kg/m^3 s
n_d, n_e, n_t	diffuse porosity, effective porosity, total porosity
P_g, P_l	gas pressure, liquid pressure, Pa
P_{cap}, P_{sat}, P_v	capillary pressure, saturation pressure, vapor pressure, Pa
$\dot{q}$	thermal energy source, W/m^3
$\dot{R}_c$	species decay rate, 1/s
R_l	liquid-phase gas constant, J/kg K
$\dot{s}_c$	species source, (mol,Ci)/m^3 s
s_g, s_l	gas saturation, liquid saturation
t	time, s
T	temperature,°C or K
u_g, u_l, u_s	gas internal energy, liquid internal energy, solid internal energy, J/kg K
V_g, V_l	gas Darcy velocity vector, liquid Darcy velocity vector, m/s
x_a, x_w	gas-phase air mass fraction, gas-phase water mass fraction
y_a, y_w	liquid-phase air mass fraction, liquid-phase water mass fraction
z	vertical height, m

Greek Characters

η_d	extended diffuse porosity
μ_g, μ_l	gas viscosity, liquid viscosity, Pa s
ρ_g, ρ_l	gas density, liquid density, kg/m^3
τ_g, τ_l	gas tortuosity, liquid tortuosity

Mathematical Symbols

~	tensor
$\hat{z}$	unit vector
∂	partial derivative
∇	gradient
[[x , y]]	maximum function

Subscripts

b,m,f	bulk, matrix, fracture properties

References

Amter, S., E. Behl, and B. Ross. 1988. *Carbon-14 Travel Time at Yucca Mountain.* Disposal Safety Incorporated, Washington, D.C.

ASME Steam Tables. 1967. *Thermodynamic and Transport Properties of Steam.* The American Society of Mechanical Engineers. United Engineering Center, New York, New York.

Carsel, R. F., and R. S. Parrish. 1988. "Developing Joint Probability Distributions of Soil Water Retention Characteristics." *Water Resources Res.* 24(5).

DOE. 1988. "Site Characterization Plan, Yucca Mountain Site, Nevada Research and Development Area, Nevada." DOE/RW-0199, Volume II, Part A, Office of Civilian Radioactive Waste Management, U.S. Department of Energy, Washington, D.C.

Millington, R. J., and J. P. Quirk. 1959. "Permeability of Porous Media." *Nature* 183: 387-388.

Montazer, P., and W. E. Wilson. 1984. *Conceptual Hydrologic Model of Flow in the Unsaturated Zone, Yucca Mountain, Nevada.* U.S. Geological Survey Water Resources Investigation Report 84-4345, U.S. Geological Survey, Denver, Colorado.

Nitao, J. J. 1988. *Numerical Modeling of the Thermal and Hydrological Environment Around a Nuclear Waste Package Using Equivalent Continuum Approximation: Horizontal Emplacement.* UCID-21444, Lawrence Livermore National Laboratory, Livermore, California.

Nitao, J. J., and T. A. Buscheck. 1989. *Movement of a Liquid Front in an Unsaturated, Fractured Porous Medium, 1, Physical Theory.* UCRL-101005, Lawrence Livermore National Laboratory, Livermore, California.

Nitao, J. J. 1989. *Movement of a Liquid Front in an Unsaturated, Fractured Porous Medium, 2, Mathematical Analysis.* UCRL-101006, Lawrence Livermore National Laboratory, Livermore, California.

Patankar, S. V. 1980. *Numerical Heat Transfer and Fluid Flow.* Hemisphere Publishing Corporation, Washington D.C.

Peters, R. R., and E. A. Klavetter. 1988. "A Continuum Model for Water Movement in an Unsaturated Fractured Rock Mass." *Water Resour. Res.* 24(3): 416-430.

Peters, R. R., E. A. Klavetter, I. J. Hall, S. C. Blair, P. R. Heller, and G. W. Gee. 1984. *Fracture and Matrix Hydrogeologic Characteristics of Tuffaceous Materials from Yucca Mountain, Nye County, Nevada.* SAND84-1471, Sandia National Laboratories, Albuquerque, New Mexico.

Ross, B. 1988. "Gas-Phase Transport of Carbon-14 Released From Nuclear Waste into the Unsaturated Zone." *Scientific Basis of Nuclear Waste Management XI*, pp. 273-284, M.J. Apted and R.E. Westerman, eds. Materials Research Society, Pittsburgh.

Schelling, F. J. 1987. *The NNWSI Project Reference Information Base Version 02.001.* SLTR87-6001.

Spengler, R., M. Chornack, D. C. Muller, and J. E. Kibler. 1984. *Stratigraphic and Structural Characteristics of Volcanic Rocks in Core Hole USW G-4, Yucca Mountain, Nye County, Nevada.* U. S. Geological Survey Open File Report 84-789.